

***Ab initio* and Vibrational Predissociation Studies on Methylammonium-(Water)₄ Complex: Evidence for Multiple Cyclic and Non-cyclic Hydrogen-bonded Structures**

Kwang-Yon Kim, Woon-Hui Han, Ung-In Cho, Yuan T. Lee,[†] and Doo Wan Boo^{*}

Department of Chemistry, Yonsei University, Seoul 120-749, Korea. *E-mail: dwboo@yonsei.ac.kr
[†]Institute of Atomic and Molecular Sciences, Academia Sinica, P.O. Box 23-166, Taipei, Taiwan, R.O.C
Received October 26, 2006

The combined *ab initio* and vibrational predissociation (VP) spectroscopic studies on methylammonium-(water)₄ complex aimed at understanding the hydration behavior of an amphiphilic ion core are described. The *ab initio* calculations predicted eleven low-energy isomers forming cyclic, tripod, chain, and caged structures, and their relative stabilities, total hydration energies and thermodynamic functions at 298 K and 150 K. The excellent correlation between the observed VP spectra and *ab initio* spectra for bonded N-H, bonded O-H and free O-H stretches suggested co-existence of five cyclic isomers and two non-cyclic isomers in ion beam at 150 K, consistent with the trends of calculated Gibbs free energies.

Key Words : Methylammonium-(water)₄, *Ab initio*, Vibrational predissociation, Hydrogen bonding, Cyclic isomers

Introduction

The solvation structures and dynamics of protonated ions in water play an important role in many chemical and biological processes.^{1,2} The ion hydration processes in the first few solvation shells are of particular importance in determining the conformations and activities of biomolecules.^{3,4} The hydrogen bond (HB) networks close to the ionic chromophores are generally governed by the competition between ion-water and water-water interactions, different from those in the bulk where the water-water interactions are dominant. During the past few decades, the *ab initio* theoretical,^{5,6} gas phase mass spectrometric,^{7,8} and spectroscopic⁹ studies on size-selected, protonated ion-water complexes have provided a detailed understanding on ion-water and water-water interactions, and on the structural evolution with increasing number of water molecules.

Methylammonium-(water)₄ (or CH₃NH₃⁺(H₂O)₄) complex is of particular interest in that methylammonium (Ma) core is the simplest model for the N-terminal groups of amino acids, peptides and proteins. It is also the smallest Ma(H₂O)_n complex containing one excess water molecule than the number of protons in Ma core which permits the study of the HB landscape just outside the first hydration shell (denoted as 1^oH₂O) where ion-water and water-water interactions strongly compete. Moreover, due to the amphiphilic nature of Ma core containing the hydrophilic (-NH₃⁺) and hydrophobic (-CH₃) moieties, it is expected that the HB networks formed around Ma core are somewhat different from those of hydrophilic ion cores such as NH₄⁺, H₃O⁺, etc.^{10,11}

In this paper we report the combined *ab initio* theoretical and VP spectroscopic studies on the structures, interactions and vibrations of Ma(H₂O)₄ complex aimed at understanding the hydration behavior of an amphiphilic ion core. It will be shown later that Ma(H₂O)₄ complex adopt multiple cyclic and non-cyclic structures at 150 K unlike the case of

NH₄⁺(H₂O)₄ complex. The correlation between the experimentally observed VP spectra and *ab initio* calculated spectra is elaborately discussed.

Methodology

***Ab initio* quantum calculations.** *Ab initio* quantum computations on Ma(H₂O)₄ at B3LYP/6-31+G(d) and B3LYP/6-311++G(d,p) levels were performed using the Gaussian-98 program.¹² The geometries were optimized using analytical gradients at B3LYP/6-31+G(d) and the vibrational frequencies were obtained using analytical second derivatives at B3LYP/6-31+G(d) and B3LYP/6-311++G(d,p) levels. The scaling factors for the calculated frequencies at B3LYP/6-31+G(d) and B3LYP/6-311++G(d,p) were 0.973, 0.979 determined by referring to the experimentally observed symmetric free O-H stretch frequency. The calculated total hydration energies, enthalpies and Gibbs free energies were corrected by zero-point vibrational energy (ZPVE) and basis set superposition errors (BSSE) following the procedures of Boys-Bernardi.¹³

Vibrational predissociation spectroscopy. The experiment was conducted using a vibrational predissociation ion trap (VPIT) spectrometer. Details of the apparatus have been previously described.¹⁴ Briefly, we synthesized Ma(H₂O)₄ ions by a low current, low temperature corona discharge of CH₃NH₂/H₂O gas mixture seeded in pure H₂ at the pressure of ~150 torr, and subsequent supersonic expansion. The rotational and vibrational temperatures were estimated to be ~50 K and ~150 K, respectively. The Ma(H₂O)₄ ions were mass-selected by a sector magnet and then stored in an octapole ion trap for ~1 ms before infrared irradiation. A quadrupole mass spectrometer equipped with a Daly detector operated in ion counting modes, selectively detected the fragment ions, Ma(H₂O)₃ upon infrared irradiation to obtain virtually background-free spectra. The excitation was made

by a pulsed infrared laser, generated by difference frequency mixing of Nd-YAG laser and dye laser photons. Since the hydration enthalpy by fourth H₂O molecule in Ma(H₂O)₄ is ~10 kcal/mol,¹⁵ one or two infrared photons in the range of 2750-3850 cm⁻¹ used in this work are sufficient to dissociate Ma(H₂O)₄ into Ma(H₂O)₃ and one H₂O molecule. The ion signal of Ma(H₂O)₃ measured as a function of IR frequency represents the infrared spectrum of the parent ion complex, Ma(H₂O)₄.

Results and Discussion

Ab initio geometries and energetics. Among a number of low-lying structural isomers optimized at B3LYP/6-31+G(d) level, the lowest eleven isomers numbered in the order of the BSSE- and ZPVE-corrected electronic energies are depicted in Figure 1 and their selected geometrical parameters listed in Table 1. They exhibit several distinct structural characteristics. Four water molecules in the eleven isomers are bonded exclusively to the -NH₃⁺ hydrophilic moiety of Ma core, and the isomers with water molecules attached to the -CH₃ hydrophobic moiety were predicted to be much higher in energy. Such asymmetric hydration around amphiphilic protonated chromophores have been reported previously.¹⁵

Depending on the shapes of hydrated structures, they can be classified to the cyclic isomers (I, II, III, VI, VII, IX, XI), tripod isomer (IV), chain isomers (V, VIII), and caged isomer (X). Among these isomers, four isomers (I, IV, IX, X) contain three ion-water HB's between -NH₃⁺ moiety and 1^o H₂O molecules, and others (II, III, V, VI, VII, VIII, XI) have two ion-water HB's and one additional water-water HB. Owing to the superior strengths of charge-dipole interactions (bond energy = ~18 kcal/mol) vs. water-water HB interactions (bond energy = ~4 kcal/mol),¹⁷ facile rearrangements among the isomers with the same numbers of ion-water HB's are expected to occur *via* simple rupture/formation of water-water HB's and migration of water molecules.

The calculated electronic energies for isomers I-XI and total hydration energies for the clustering reaction CH₃NH₃⁺ + 4H₂O → CH₃NH₃⁺(H₂O)₄ at B3LYP/6-31+G(d) and B3LYP/6-311++G(d,p) levels with and without ZPVE- and BSSE-corrections are listed in Table 2. In the following the B3LYP/6-311++G(d,p) results are mainly discussed. Having cyclic HB network and more ion-water HB's are generally advantageous for forming stable structures, but the extent of strains in the cyclic HB network and the hydrogen bond cooperativity play important roles in determining their overall stabilities. The cyclic isomers I and IX, for instance, contain four-membered HB (4-HB) ring and three ion-water HB's, but isomer I is the global minimum energy structure while isomer IX is ~3 kcal/mol higher in energy than isomer I. The energy difference is attributed to the large 4-HB ring strains in isomer IX arising from the changes in the HB roles of H₂O(1) and H₂O(4). Note that the H₂O(1) and H₂O(4) in isomer I play roles of a proton acceptor and donor (Ad) and a proton double acceptor (aa), respectively while their HB roles are switched in isomer IX.¹⁸ These result in the inhomogeneous HB lengths, the steeper HB angles and the distorted HB ring for isomer IX compared to those of isomer I (for instance, R(H_N¹O₁)_{IX} = 2.01 Å, R(H_N²O₂)_{IX} = 1.74 Å, R(H_N¹O₁)_I = R(H_N²O₂)_I = 1.81 Å, ∠(O₂H₂⁴O₄)_{IX} = 148.4°, ∠(O₂H₂⁴O₄)_I = 161.9°, D(NO₁O₂O₄)_{IX} = -111.4°, D(NO₁O₂O₄)_I = 178.2°).

The slight energy difference (~0.3 kcal/mol) between isomer I and isomers II, III having only two ion-water HB's suggests the importance of the HB cooperative effects for the latter evidenced by the shortened ion-water and water-water HB's for isomers II, III vs. I (e.g. R(H_N¹O₁)_{II,III} = 1.74 Å, R(H_N¹O₁)_I = 1.81 Å, R(H_{1,2}³O₃)_{II,III} = 1.84 Å, R(H_{1,2}⁴O₄)_I = 1.93 Å). Note that isomers II, III are even lower in energy than isomer I without the BSSE- and ZPVE-corrections (Table 2). For isomer VI, the asymmetric binding of H₂O(4) to the 4-HB ring modifies the HB role of H₂O(2) to a proton single acceptor and double donor (Add) different from those of isomers II, III. The unequal HB roles

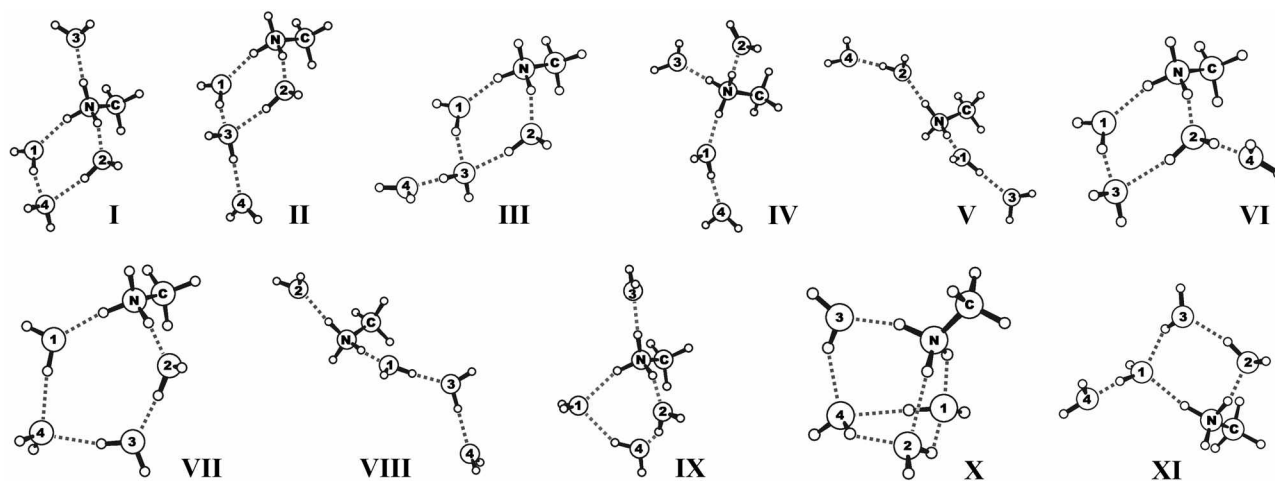


Figure 1. *Ab initio* optimized structures of CH₃NH₃⁺(H₂O)₄ at B3LYP/6-31+G(d). The numbers on oxygen atom indicate no. of water molecules in the complex.

Table 1. Selected geometrical parameters for isomers I-XI of $\text{CH}_3\text{NH}_3^+(\text{H}_2\text{O})_4$ at B3LYP/6-31+G(d).^a Distances (R) are in angstroms, angles (\angle) and dihedral angles (D) are in degrees

Isomers	Geometrical Parameters
I	$R(\text{NO}_{1,2}) = 2.81$, $R(\text{NO}_3) = 2.87$, $R(\text{O}_{1,2}\text{O}_4) = 2.88$, $R(\text{H}_N^1\text{O}_1) = R(\text{H}_N^2\text{O}_2) = 1.81$, $R(\text{H}_N^3\text{O}_3) = 1.84$, $R(\text{H}_{1,2}^4\text{O}_4) = 1.93$, $\angle(\text{H}_N^1\text{NH}_N^2) = 104.6$, $\angle(\text{H}_N^1\text{NH}_N^3) = 109.2$, $\angle(\text{O}_1\text{NO}_2) = 81.5$, $\angle(\text{O}_{1,2}\text{NO}_3) = 119.9$, $\angle(\text{CNO}_4) = 122.2$, $\angle(\text{NH}_N^1\text{O}_1) = \angle(\text{NH}_N^2\text{O}_2) = 161.1$, $\angle(\text{NH}_N^3\text{O}_3) = 173.9$, $\angle(\text{O}_1\text{H}_1^4\text{O}_4) = \angle(\text{O}_2\text{H}_2^4\text{O}_4) = 161.9$, $\angle(\text{H}_1^4\text{O}_4\text{H}_2^4) = 91.4$, $D(\text{NO}_1\text{O}_2\text{O}_4) = 178.2$
II	$R(\text{NO}_{1,2}) = 2.75$, $R(\text{O}_{1,2}\text{O}_3) = 2.80$, $R(\text{O}_3\text{O}_4) = 2.74$, $R(\text{H}_N^1\text{O}_1) = R(\text{H}_N^2\text{O}_2) = 1.74$, $R(\text{H}_{1,2}^3\text{O}_3) = 1.84$, $R(\text{H}_3^4\text{O}_4) = 1.75$, $\angle(\text{H}_N^1\text{NH}_N^2) = 104.3$, $\angle(\text{H}_N^1\text{NH}_N^3) = 108.4$, $\angle(\text{O}_1\text{NO}_2) = 82.0$, $\angle(\text{CNO}_4) = 106.1$, $\angle(\text{NH}_N^1\text{O}_1) = \angle(\text{NH}_N^2\text{O}_2) = 161.8$, $\angle(\text{O}_1\text{H}_1^3\text{O}_3) = \angle(\text{O}_2\text{H}_2^3\text{O}_3) = 162.9$, $\angle(\text{O}_3\text{H}_3^4\text{O}_4) = 179.2$, $\angle(\text{H}_1^3\text{O}_3\text{H}_2^3) = 92.2$, $D(\text{NO}_1\text{O}_2\text{O}_3) = 177.0$
III	$R(\text{NO}_{1,2}) = 2.75$, $R(\text{O}_{1,2}\text{O}_3) = 2.80$, $R(\text{O}_3\text{O}_4) = 2.75$, $R(\text{H}_N^1\text{O}_1) = R(\text{H}_N^2\text{O}_2) = 1.74$, $R(\text{H}_{1,2}^3\text{O}_3) = 1.84$, $R(\text{H}_3^4\text{O}_4) = 1.76$, $\angle(\text{H}_N^1\text{NH}_N^2) = 104.3$, $\angle(\text{H}_N^1\text{NH}_N^3) = 108.4$, $\angle(\text{O}_1\text{NO}_2) = 82.1$, $\angle(\text{CNO}_4) = 145.0$, $\angle(\text{NH}_N^1\text{O}_1) = \angle(\text{NH}_N^2\text{O}_2) = 161.8$, $\angle(\text{O}_1\text{H}_1^3\text{O}_3) = \angle(\text{O}_2\text{H}_2^3\text{O}_3) = 162.6$, $\angle(\text{O}_3\text{H}_3^4\text{O}_4) = 179.7$, $\angle(\text{H}_1^3\text{O}_3\text{H}_2^3) = 92.4$, $D(\text{NO}_1\text{O}_2\text{O}_3) = 177.8$
IV	$R(\text{NO}_1) = 2.79$, $R(\text{NO}_{2,3}) = 2.88$, $R(\text{O}_1\text{O}_4) = 2.77$, $R(\text{H}_N^1\text{O}_1) = 1.74$, $R(\text{H}_N^2\text{O}_2) = R(\text{H}_N^3\text{O}_3) = 1.84$, $R(\text{H}_1^4\text{O}_4) = 1.78$, $\angle(\text{H}_N^1\text{NH}_N^2) = 108.3$, $\angle(\text{H}_N^1\text{NH}_N^3) = 108.1$, $\angle(\text{H}_N^2\text{NH}_N^3) = 108.1$, $\angle(\text{O}_1\text{NO}_2) = 112.1$, $\angle(\text{O}_1\text{NO}_3) = 109.3$, $\angle(\text{O}_2\text{NO}_3) = 109.3$, $\angle(\text{CNO}_4) = 82.1$, $\angle(\text{NH}_N^1\text{O}_1) = \angle(\text{NH}_N^2\text{O}_2) = 175.9$, $\angle(\text{NH}_N^3\text{O}_3) = 178.1$, $D(\text{O}_4\text{O}_1\text{NC}) = -27.1$
V	$R(\text{NO}_{1,2}) = 2.76$, $R(\text{O}_1\text{O}_3) = R(\text{O}_2\text{O}_4) = 2.76$, $R(\text{H}_N^1\text{O}_1) = R(\text{H}_N^2\text{O}_2) = 1.71$, $R(\text{H}_N^3\text{O}_3) = R(\text{H}_1^4\text{O}_4) = 1.77$, $\angle(\text{H}_N^1\text{NH}_N^2) = 109.0$, $\angle(\text{H}_N^1\text{NH}_N^3) = \angle(\text{H}_N^2\text{NH}_N^3) = 107.4$, $\angle(\text{O}_1\text{NO}_2) = 114.0$, $\angle(\text{CNO}_4) = 111.5$, $\angle(\text{NH}_N^1\text{O}_1) = 175.7$, $\angle(\text{NH}_N^2\text{O}_2) = 175.5$, $\angle(\text{O}_1\text{H}_1^3\text{O}_3) = 174.7$, $\angle(\text{O}_2\text{H}_2^4\text{O}_4) = 174.5$, $D(\text{O}_3\text{O}_1\text{NC}) = -41.1$, $D(\text{O}_4\text{O}_2\text{NC}) = 100.3$
VI	$R(\text{NO}_1) = 2.78$, $R(\text{NO}_2) = 2.71$, $R(\text{O}_1\text{O}_3) = 2.85$, $R(\text{O}_2\text{O}_3) = 2.92$, $R(\text{O}_2\text{O}_4) = 2.78$, $R(\text{H}_N^1\text{O}_1) = 1.77$, $R(\text{H}_N^2\text{O}_2) = 1.68$, $R(\text{H}_1^3\text{O}_3) = 1.91$, $R(\text{H}_2^3\text{O}_3) = 1.97$, $R(\text{H}_3^4\text{O}_4) = 1.79$, $\angle(\text{H}_N^1\text{NH}_N^2) = 104.4$, $\angle(\text{H}_N^1\text{NH}_N^3) = 108.3$, $\angle(\text{H}_N^2\text{NH}_N^3) = 108.5$, $\angle(\text{O}_1\text{NO}_2) = 84.1$, $\angle(\text{CNO}_3) = 125.6$, $\angle(\text{CNO}_4) = 106.3$, $\angle(\text{NH}_N^1\text{O}_1) = 161.2$, $\angle(\text{NH}_N^2\text{O}_2) = 165.6$, $\angle(\text{O}_1\text{H}_1^3\text{O}_3) = 161.8$, $\angle(\text{O}_2\text{H}_2^3\text{O}_3) = 159.4$, $\angle(\text{O}_2\text{H}_2^4\text{O}_4) = 178.5$, $\angle(\text{H}_1^3\text{O}_3\text{H}_2^3) = 92.0$, $D(\text{O}_4\text{O}_2\text{NC}) = 70.5$, $D(\text{O}_3\text{O}_2\text{NO}_4) = 172.5$, $D(\text{NO}_1\text{O}_2\text{O}_3) = 177.8$
VII	$R(\text{NO}_1) = 2.81$, $R(\text{NO}_2) = 2.73$, $R(\text{O}_1\text{O}_4) = 2.88$, $R(\text{O}_2\text{O}_3) = 2.73$, $R(\text{O}_3\text{O}_4) = 2.89$, $R(\text{H}_N^1\text{O}_1) = 1.77$, $R(\text{H}_N^2\text{O}_2) = 1.68$, $R(\text{H}_1^4\text{O}_4) = 1.90$, $R(\text{H}_2^3\text{O}_3) = 1.76$, $R(\text{H}_3^4\text{O}_4) = 1.94$, $\angle(\text{H}_N^1\text{NH}_N^2) = 106.8$, $\angle(\text{H}_N^1\text{NH}_N^3) = 108.0$, $\angle(\text{H}_N^2\text{NH}_N^3) = 108.1$, $\angle(\text{O}_1\text{NO}_2) = 99.9$, $\angle(\text{CNO}_3) = 104.0$, $\angle(\text{CNO}_4) = 113.8$, $\angle(\text{NH}_N^1\text{O}_1) = 174.0$, $\angle(\text{NH}_N^2\text{O}_2) = 170.4$, $\angle(\text{O}_1\text{H}_1^4\text{O}_4) = 174.4$, $\angle(\text{O}_2\text{H}_2^3\text{O}_3) = 167.3$, $\angle(\text{O}_3\text{H}_3^4\text{O}_4) = 166.0$, $\angle(\text{H}_2^3\text{O}_3\text{H}_1^4) = 97.2$, $D(\text{O}_4\text{O}_3\text{O}_2\text{N}) = -37.5$, $D(\text{O}_3\text{O}_4\text{O}_1\text{N}) = -6.5$, $D(\text{O}_2\text{O}_3\text{O}_4\text{O}_1) = 25.7$
VIII	$R(\text{NO}_1) = 2.71$, $R(\text{NO}_2) = 2.85$, $R(\text{O}_1\text{O}_3) = 2.68$, $R(\text{O}_3\text{O}_4) = 2.78$, $R(\text{H}_N^1\text{O}_1) = 1.66$, $R(\text{H}_N^2\text{O}_2) = 1.81$, $R(\text{H}_1^3\text{O}_3) = 1.70$, $R(\text{H}_2^3\text{O}_3) = 1.79$, $\angle(\text{H}_N^1\text{NH}_N^2) = 108.8$, $\angle(\text{H}_N^1\text{NH}_N^3) = 107.5$, $\angle(\text{H}_N^2\text{NH}_N^3) = 107.8$, $\angle(\text{O}_1\text{NO}_2) = 112.4$, $\angle(\text{CNO}_3) = 75.5$, $\angle(\text{CNO}_4) = 84.0$, $\angle(\text{NH}_N^1\text{O}_1) = 171.7$, $\angle(\text{NH}_N^2\text{O}_2) = 177.1$, $\angle(\text{O}_1\text{H}_1^3\text{O}_3) = 170.1$, $\angle(\text{O}_2\text{H}_2^4\text{O}_4) = 178.9$, $D(\text{O}_3\text{O}_1\text{NC}) = -32.0$, $D(\text{O}_4\text{O}_3\text{O}_1\text{N}) = -105.3$
IX	$R(\text{NO}_1) = 3.01$, $R(\text{NO}_2) = 2.75$, $R(\text{NO}_3) = 2.87$, $R(\text{O}_1\text{O}_4) = 2.88$, $R(\text{O}_2\text{O}_4) = 2.73$, $R(\text{H}_N^1\text{O}_1) = 2.01$, $R(\text{H}_N^2\text{O}_2) = 1.74$, $R(\text{H}_1^3\text{O}_3) = 1.83$, $R(\text{H}_2^3\text{O}_3) = 1.85$, $R(\text{H}_3^4\text{O}_4) = 2.01$, $\angle(\text{H}_N^1\text{NH}_N^2) = 105.6$, $\angle(\text{H}_N^1\text{NH}_N^3) = 108.8$, $\angle(\text{H}_N^2\text{NH}_N^3) = 109.1$, $\angle(\text{O}_1\text{NO}_2) = 84.3$, $\angle(\text{CNO}_4) = 85.0$, $\angle(\text{NO}_1\text{O}_4) = 71.36$, $\angle(\text{NO}_2\text{O}_4) = 77.7$, $\angle(\text{O}_1\text{O}_4\text{O}_2) = 87.1$, $\angle(\text{NH}_N^1\text{O}_1) = 162.1$, $\angle(\text{NH}_N^2\text{O}_2) = 161.2$, $\angle(\text{NH}_N^3\text{O}_3) = 177.9$, $\angle(\text{O}_2\text{H}_2^4\text{O}_4) = 148.4$, $\angle(\text{O}_4\text{H}_1^1\text{O}_1) = 147.9$, $\angle(\text{H}_1^1\text{O}_1\text{H}_1^1) = 87.3$, $D(\text{NO}_1\text{O}_2\text{O}_4) = -111.4$
X	$R(\text{NO}_1) = 2.87$, $R(\text{NO}_2) = 2.92$, $R(\text{NO}_3) = 2.75$, $R(\text{O}_1\text{O}_2) = 2.79$, $R(\text{O}_1\text{O}_4) = 2.81$, $R(\text{O}_2\text{O}_4) = 2.83$, $R(\text{O}_3\text{O}_4) = 2.80$, $R(\text{H}_N^1\text{O}_1) = 1.94$, $R(\text{H}_N^2\text{O}_2) = 2.09$, $R(\text{H}_N^3\text{O}_3) = 1.74$, $R(\text{H}_1^4\text{O}_4) = 1.96$, $R(\text{H}_2^4\text{O}_4) = 2.11$, $R(\text{H}_3^4\text{O}_4) = 1.99$, $R(\text{H}_4^4\text{O}_4) = 1.91$, $\angle(\text{H}_N^1\text{NH}_N^2) = 104.2$, $\angle(\text{H}_N^1\text{NH}_N^3) = 105.9$, $\angle(\text{H}_N^2\text{NH}_N^3) = 106.5$, $\angle(\text{O}_1\text{NO}_2) = 57.7$, $\angle(\text{O}_1\text{NO}_3) = 89.2$, $\angle(\text{O}_2\text{NO}_3) = 90.7$, $\angle(\text{CNO}_4) = 172.9$, $\angle(\text{NO}_1\text{O}_4) = 81.4$, $\angle(\text{NO}_2\text{O}_4) = 80.1$, $\angle(\text{NO}_3\text{O}_4) = 83.6$, $\angle(\text{O}_1\text{O}_2\text{O}_4) = 59.8$, $\angle(\text{O}_2\text{O}_1\text{O}_4) = 60.7$, $\angle(\text{O}_1\text{O}_4\text{O}_2) = 59.4$, $\angle(\text{O}_1\text{O}_4\text{O}_3) = 89.3$, $\angle(\text{O}_2\text{O}_4\text{O}_3) = 91.5$, $\angle(\text{NH}_N^1\text{O}_1) = 146.7$, $\angle(\text{NH}_N^2\text{O}_2) = 136.2$, $\angle(\text{NH}_N^3\text{O}_3) = 160.4$, $\angle(\text{O}_1\text{H}_1^4\text{O}_4) = 143.1$, $\angle(\text{O}_2\text{H}_2^4\text{O}_4) = 125.3$, $\angle(\text{O}_3\text{H}_3^4\text{O}_4) = 149.3$, $\angle(\text{O}_4\text{H}_4^1\text{O}_2) = 141.8$, $\angle(\text{H}_1^4\text{O}_4\text{H}_3^4) = 100.6$, $D(\text{NO}_1\text{O}_2\text{O}_4) = 96.0$
XI	$R(\text{NO}_1) = 2.87$, $R(\text{NO}_2) = 2.71$, $R(\text{O}_1\text{O}_3) = 2.87$, $R(\text{O}_1\text{O}_4) = 2.73$, $R(\text{O}_2\text{O}_3) = 2.71$, $R(\text{H}_N^1\text{O}_1) = 1.85$, $R(\text{H}_N^2\text{O}_2) = 1.67$, $R(\text{H}_1^4\text{O}_4) = 1.74$, $R(\text{H}_2^4\text{O}_4) = 1.76$, $R(\text{H}_3^4\text{O}_4) = 1.91$, $\angle(\text{H}_N^1\text{NH}_N^2) = 105.9$, $\angle(\text{H}_N^1\text{NH}_N^3) = 107.9$, $\angle(\text{H}_N^2\text{NH}_N^3) = 108.4$, $\angle(\text{O}_1\text{NO}_2) = 91.0$, $\angle(\text{CNO}_4) = 140.8$, $\angle(\text{NO}_1\text{O}_3) = 85.6$, $\angle(\text{NO}_1\text{O}_4) = 107.8$, $\angle(\text{NO}_2\text{O}_3) = 92.1$, $\angle(\text{O}_1\text{O}_3\text{O}_2) = 91.0$, $\angle(\text{NH}_N^1\text{O}_1) = 167.7$, $\angle(\text{NH}_N^2\text{O}_2) = 166.0$, $\angle(\text{O}_1\text{H}_1^4\text{O}_4) = 171.1$, $\angle(\text{O}_2\text{H}_2^3\text{O}_3) = 159.9$, $\angle(\text{O}_3\text{H}_3^4\text{O}_4) = 155.8$, $\angle(\text{H}_N^1\text{O}_1\text{H}_N^1) = 96.9$, $D(\text{NO}_1\text{O}_2\text{O}_4) = -174.2$, $D(\text{O}_4\text{O}_1\text{O}_3\text{O}_2) = 111.3$

^aThe subscripts of O atoms denote no. of oxygen atoms according to Figure 1. The subscripts and superscripts of H atoms denote the covalently bonded atoms and hydrogen-bonded atoms, respectively.

Table 2. Electronic energies and total hydration energies of isomers **I-XI** of CH₃NH₃⁺(H₂O)₄ at B3LYP/6-31+G(d) and B3LYP/6-311++G(d,p). All the absolute energies are in hartree, and the relative energies in parentheses and total hydration energies are in kcal/mol

	B3LYP/6-31+G(d)				B3LYP/6-311++G(d,p)			
	<i>E_{el}</i>	<i>E_{el}</i> ^a	<i>E_{el}</i> ^b	Δ <i>E</i> ^b	<i>E_{el}</i>	<i>E_{el}</i> ^a	<i>E_{el}</i> ^b	Δ <i>E</i> ^b
I	-402.011745 (0.39)	-402.003365 (0.07)	-401.830800 (0.00)	-55.64	-402.188932 (0.05)	-402.182822 (0.00)	-402.007045 (0.00)	-52.04
II	-402.012323 (0.03)	-402.003443 (0.02)	-401.830324 (0.30)	-55.34	-402.188975 (0.02)	-402.182576 (0.15)	-402.006515 (0.33)	-51.71
III	-402.012368 (0.00)	-402.003473 (0.00)	-401.830257 (0.34)	-55.30	-402.189010 (0.00)	-402.182611 (0.13)	-402.006487 (0.35)	-51.69
IV	-402.008039 (2.72)	-402.000482 (1.88)	-401.830105 (0.44)	-55.21	-402.186214 (1.76)	-402.180497 (1.46)	-402.006072 (0.61)	-51.43
V	-402.007737 (2.91)	-401.999885 (2.25)	-401.828465 (1.47)	-54.18	-402.185613 (2.13)	-402.179663 (1.98)	-402.004775 (1.42)	-50.62
VI	-402.009564 (1.76)	-402.000903 (1.61)	-401.827984 (1.77)	-53.87	-402.186670 (1.47)	-402.180364 (1.54)	-402.004492 (1.60)	-50.44
VII	-402.010040 (1.46)	-402.001116 (1.48)	-401.827792 (1.89)	-53.75	-402.186869 (1.34)	-402.180488 (1.46)	-402.004441 (1.63)	-50.41
VIII	-402.005668 (4.20)	-401.997781 (3.57)	-401.826427 (2.74)	-52.90	-402.183357 (3.55)	-402.177408 (3.40)	-402.002576 (2.80)	-49.24
IX	-402.007170 (3.26)	-401.999070 (2.76)	-401.826233 (2.87)	-52.78	-402.184037 (3.12)	-402.177955 (3.05)	-402.002218 (3.03)	-49.01
X	-402.010405 (1.23)	-402.001729 (1.09)	-401.826489 (2.71)	-52.84	-402.185655 (2.11)	-402.179406 (2.14)	-402.002133 (3.08)	-48.96
XI	-402.007837 (2.84)	-401.998883 (2.88)	-401.825094 (3.58)	-52.06	-402.184030 (3.12)	-402.177404 (3.40)	-402.001281 (3.62)	-48.43

^aBSSE-corrected. ^bBSSE- and ZPVE-corrected

of H₂O(1,2) increase the inhomogeneity of HB lengths resulting in some instability (~1.3 kcal/mol) for isomer **VI** (Table 1). The five-membered HB (5-HB) ring isomer (**VII**) can be viewed as an intermediate for isomerization reactions (**II** → **V**, **V** → **VIII**). It is ~1.6 kcal/mol higher in energy than isomer **I** due to the asymmetric HB roles of 2° H₂O(3,4) (Ad. aa). The cyclic isomer **XI** and the caged isomer **X** are much higher in energy due to the combined ring strains and inefficient charge-dipole interactions.

The tripod isomer (**IV**) and chain isomers (**V**, **VIII**) can be formed *via* simple bond rupture of 4-, 5-HB rings from the corresponding cyclic isomers (**I** and **VI**, **VII**, respectively), resulting in one less water-water HB but with less strains in the HB network compared to the cyclic isomers. The fact that isomer **IV** is only ~0.6 kcal/mol higher in energy than **I** and that isomer **V** is ~0.2 kcal/mol lower in energy than **VII** despite the energy deficit of one water-water HB (~4 kcal/mol) suggests the importance of geometrically relaxed local HB environments. Finally, the energy difference (~1.4 kcal/mol) between symmetric chain isomer (**V**) and asymmetric chain isomer (**VIII**) is attributed to the greater indirect charge-dipole interactions for 2° H₂O vs. 3° H₂O.

Compared with the previous results on NH₄⁺(H₂O)₄,¹⁰ the energy differences between isomers **I-XI** for Ma(H₂O)₄ somewhat decreased due to the weaker charge-dipole interactions for the latter resulting from the reduced charge densities of protons by methyl substitution. Of notice is the existence of multiple cyclic isomers with lower energies

within 2 kcal/mol (**I**, **II**, **III**, **VI**, **VII**) besides non-cyclic isomers, different from the cases of NH₄⁺(H₂O)₄ that one cyclic (**I**) and two non-cyclic isomers are predominant.^{10,11} In particular, the energy differences between isomers **II**, **III** and **I** (0.34 kcal/mol) are predicted to be lower than the corresponding values for NH₄⁺(H₂O)₄ (1.15 kcal/mol) at B3LYP/6-311++G(d,p) level. Moreover, the other cyclic isomers (**VI**, **VII**) were not reported previously in the case of NH₄⁺(H₂O)₄.^{10,11} Another discrepancy is that isomer **I** is the second lowest energy isomer for NH₄⁺(H₂O)₄ next to the non-cyclic isomer having four ion-water HB's.^{10,11} Therefore, the existence of multiple stable cyclic and non-cyclic isomers (**I-VII**) for Ma(H₂O)₄ may hint at the diverse hydration landscapes around amphiphilic ion cores.

Hydration energies and thermodynamics. As shown in Table 2, the total hydration energies for isomers **I-XI** at B3LYP/6-311++G(d,p) level are in the range of -48.4 ~ -52.0 kcal/mol. These values are 4 ~ 5 kcal/mol smaller than those of NH₄⁺(H₂O)₄¹⁰ due to the decreased charge densities of protons by methyl substitution. The stepwise hydration energies for the fourth water binding, *i.e.* CH₃NH₃⁺(H₂O)₃ + H₂O → CH₃NH₃⁺(H₂O)₄ vary in a wide range of -6.9 ~ -11.5 kcal/mol depending on the structural isomers. These results suggest the significant role of local HB interactions in determining the hydration energies of structural isomers.

The calculated total hydration enthalpies (Δ*H*_{hyd}) and total hydration Gibbs free energies (Δ*G*_{hyd}) for isomers **I-XI** at 298 K and 150 K are listed in Table 3. The calculated

Table 3. BSSE-corrected total hydration enthalpies and Gibbs free energies for isomer **I-XI** of $\text{CH}_3\text{NH}_3^+(\text{H}_2\text{O})_4$ at B3LYP/6-31+G(d) and B3LYP/6-311++G(d,p). Values in parentheses are the relative energies with respect to each minima. All values are in kcal/mol

	B3LYP/6-31+G(d)				B3LYP/6-311++G(d,p)			
	at T = 298 K		at T = 150 K		at T = 298 K		at T = 150 K	
	ΔH	ΔG	ΔH	ΔG	ΔH	ΔG	ΔH	ΔG
I	-57.19 (0.07)	-24.36 (2.75)	-57.83 (0.00)	-40.92 (0.83)	-54.88 (0.00)	-18.26 (0.73)	-54.90 (0.00)	-36.54 (0.00)
II	-57.26 (0.00)	-23.97 (3.14)	-57.62 (0.20)	-40.68 (1.08)	-54.84 (0.04)	-17.71 (1.29)	-54.65 (0.25)	-36.17 (0.36)
III	-57.25 (0.01)	-23.75 (3.36)	-57.60 (0.23)	-40.56 (1.20)	-54.84 (0.05)	-17.66 (1.34)	-54.63 (0.26)	-36.14 (0.40)
IV	-55.87 (1.39)	-27.11 (0.00)	-56.88 (0.95)	-41.76 (0.00)	-53.81 (1.07)	-19.00 (0.00)	-54.06 (0.84)	-36.44 (0.09)
V	-55.43 (1.83)	-25.89 (1.22)	-56.13 (1.70)	-40.83 (0.92)	-53.29 (1.59)	-17.95 (1.05)	-53.33 (1.57)	-35.59 (0.95)
VI	-55.71 (1.55)	-22.44 (4.67)	-56.15 (1.67)	-39.17 (2.59)	-53.44 (1.45)	-16.68 (2.31)	-53.32 (1.58)	-34.98 (1.55)
VII	-55.79 (1.47)	-22.15 (4.96)	-56.13 (1.69)	-39.03 (2.72)	-53.52 (1.36)	-16.35 (2.64)	-53.34 (1.56)	-34.84 (1.70)
VIII	-54.12 (3.14)	-24.51 (2.60)	-54.79 (3.04)	-39.48 (2.28)	-51.92 (2.96)	-16.67 (2.33)	-51.94 (2.95)	-34.26 (2.27)
IX	-54.50 (2.76)	-21.32 (5.79)	-55.06 (2.77)	-38.04 (3.72)	-51.89 (2.99)	-15.27 (3.73)	-51.86 (3.03)	-33.53 (3.00)
X	-55.71 (1.55)	-18.78 (8.33)	-55.78 (2.05)	-37.22 (4.53)	-52.45 (2.43)	-13.75 (5.25)	-52.10 (2.80)	-32.95 (3.59)
XI	-54.37 (2.88)	-20.23 (6.89)	-54.58 (3.24)	-37.32 (4.43)	-51.67 (3.21)	-14.37 (4.63)	-51.39 (3.50)	-32.89 (3.64)

thermodynamic functions at 298 K are expected to correlate with the thermodynamic values measured in high-pressure mass spectrometry,¹⁵ and the results at 150 K (vibrational temperature of our ion beam) can be used in interpreting the VP spectrum of $\text{Ma}(\text{H}_2\text{O})_4$ complex generated in supersonic ion beam condition. As shown in Table 3, the total hydration enthalpies (ΔH_{hyd}) for isomers **I-XI** at B3LYP/6-311++G(d,p) are ranged in $-51.7 \sim -54.9$ kcal/mol at 298 K. The average ΔH_{hyd} value for seven low-lying isomers (**I-VII**) is calculated to be -54.1 kcal/mol in close proximity to the experimental value (-54.0 kcal/mol).¹⁵

The total hydration Gibbs free energies (ΔG_{hyd}) at 298 K are predicted to be in the range of $-13.8 \sim -19.0$ kcal/mol, and the corresponding values at 150 K are $-32.9 \sim -36.5$ kcal/mol (Table 3). It is expected that the tripod and chain isomers (**IV**, **V**, **VIII**) have greater entropy contributions to ΔG_{hyd} than the cyclic isomers due to their open flexible structures. It is also noticeable that the tripod isomer **IV** has lowest ΔG_{hyd} at 298 K while at 150 K, isomer **I** has lowest ΔG_{hyd} owing to the decreased entropy contributions. Since seven low-lying isomers (**I-VII**) have lower ΔG_{hyd} values within 2 kcal/mol at 150 K, they would be mostly populated in our cold ion beam and contribute predominantly to the observed VP spectrum.

Vibrational predissociation and *ab initio* predicted spectra. Table 4 lists the harmonic frequencies, the IR intensities and the vibrational assignments for five types of

stretch vibrations: free O-H (f-OH), bonded O-H (b-OH), free N-H (f-NH), bonded N-H (b-NH), and C-H stretches. Among these vibrations, the C-H stretches are very weak in intensity (≤ 30 km/mol) compared to the O-H, N-H stretches except for some coupled modes to b-NH stretches. They are expected to be almost invisible in the spectra although they would appear at similar resonant frequencies as those of free methylammonium due to the asymmetric hydration around the $-\text{NH}_3^+$ moiety. Therefore, the four types of stretches (f-OH, b-OH, f-NH, b-NH) of seven low-lying isomers (**I-VII**) as mentioned previously contribute predominantly to the observed VP spectrum obtained at 150 K. As shown in Table 4, the b-OH and b-NH stretches are predicted to have greater IR intensities than f-OH and f-NH stretches, and the resonant frequencies, much red-shifted from those of isolated H_2O and CH_3NH_3^+ , are distributed in a wide frequency range due to the diverse local HB interactions in isomers **I-VII**.

Bonded N-H stretches: Figure 2 shows the observed VP spectrum and calculated stick spectra for isomers **I-VII** for $\text{Ma}(\text{H}_2\text{O})_4$ in the frequency range of $2750\text{--}3250$ cm^{-1} . The intense vibrational features were assigned exclusively to the b-NH stretches although this frequency region corresponds to the region for both b-NH and CH stretches. Several peaks are identified in the observed VP spectrum: 2818, ~ 2840 (br), 2906, ~ 2972 (br), 3049, 3075(sh), 3110(sh), 3154, 3196(sh). Note that the resonant frequencies for broad (br) features

Table 4. Scaled frequencies (cm^{-1}), IR absorption intensities (km/mol), and assignments for C-H, N-H and O-H stretches of isomer **I-XI** at B3LYP/6-311++G(d,p). Numbers in parentheses next to OH indicate no. of the corresponding water molecules in the complex. Numbers in parentheses next to NH indicate no. of hydrogen-bonded water molecules to the N-H bond

	Frequency	Intensity	Assignments
I	3731.8	126.4	antisymmetric free-OH(3) [A]
	3713.4	25.1	symmetric free-OH(1,2) [Ad,Ad]
	3710.8	257.5	antisymmetric free-OH(1,2) [Ad,Ad]
	3708.3	133.9	antisymmetric free-OH(4) [aa]
	3642.1	38.8	symmetric free-OH(3) [A]
	3623.3	18.0	symmetric free-OH(4) [aa]
	3514.3	572.6	symmetric bonded-OH(1,2) [Ad,Ad]
	3490.0	265.4	antisymmetric bonded-OH(1,2) [Ad,Ad]
	3169.0	872.8	bonded-NH(3)
	3115.7	513.3	symmetric bonded-NH(1,2)
	3112.4	485.2	antisymmetric bonded-NH(1,2)
	3076.6	13.7	asymmetric CH_3
	3073.1	23.8	asymmetric CH_3
	2988.6	14.1	symmetric CH_3
	II	3740.2	130.3
3713.4		12.5	symmetric free-OH(1,2) [Ad,Ad]
3711.3		238.9	antisymmetric free-OH(1,2) [Ad,Ad]
3681.3		96.4	free-OH(3) [aad]
3647.8		35.5	symmetric free-OH(4) [a]
3428.9		463.3	symmetric bonded-OH(1,2) [Ad,Ad]
3392.2		73.8	free-NH
3374.3		503.8	antisymmetric bonded-OH(1,2) [Ad,Ad]
3302.0		1298.8	bonded-OH(3) [aad]
3080.4		0.6	asymmetric CH_3
3075.8		0.0	asymmetric CH_3
3010.2		828.0	symmetric bonded-NH(1,2)
2986.1		206.5	symmetric CH_3
2976.1		634.4	antisymmetric bonded-NH(1,2)
IV		3738.0	121.4
	3732.0	128.1	antisymmetric free-OH(3) [A]
	3731.6	115.4	antisymmetric free-OH(2) [A]
	3709.8	103.7	free-OH(1) [Ad]
	3645.0	28.3	symmetric free-OH(4) [a]
	3642.1	27.6	symmetric (symmetric free-OH(2) + symmetric free-OH(3)) [A,A]
	3641.7	51.9	antisymmetric (symmetric free-OH(2) + symmetric free-OH(3)) [A,A]
	3376.6	724.0	bonded-OH(1) [Ad]
	3173.1	783.7	antisymmetric bonded-NH(2,3)
	3152.8	518.1	symmetric bonded-NH(2,3)
	3074.2	8.5	asymmetric CH_3
	3073.3	4.0	asymmetric CH_3
	3007.7	902.1	bonded-NH(1)
	2984.8	140.2	symmetric CH_3
	V	3736.9	125.9
3736.5		117.2	antisymmetric free-OH(3) [a]
3709.7		139.8	symmetric free-OH(1,2) [Ad,Ad]
3709.3		74.7	antisymmetric free-OH(1,2) [Ad,Ad]
3644.2		25.3	symmetric free-OH(4) [a]
3643.8		36.2	symmetric free-OH(3) [a]

Table 4. Continued

	Frequency	Intensity	Assignments
	3388.1	85.8	free-NH
	3360.5	206.2	symmetric bonded-OH(1,2) [Ad,Ad]
	3357.4	1339.2	antisymmetric bonded-OH(1,2) [Ad,Ad]
	3078.5	0.9	asymmetric CH_3
	3076.0	0.1	asymmetric CH_3
	2992.1	16.7	symmetric CH_3
	2946.3	603.2	symmetric bonded-NH(1,2)
	2935.3	1886.0	antisymmetric bonded-NH(1,2)
VI	3742.4	119.7	antisymmetric free-OH(4) [a]
	3711.5	138.9	free-OH(1) [Ad]
	3710.7	128.4	antisymmetric free-OH(3) [aa]
	3645.4	21.1	symmetric free-OH(4) [a]
	3626.8	17.0	symmetric free-OH(3) [aa]
	3569.0	574.8	bonded-OH(2) \cdots O3 [Add]
	3477.3	474.9	bonded-OH(1) [Ad]
	3411.9	647.9	bonded-OH(2) \cdots O4 [Add]
	3393.6	88.4	free-NH
	3079.3	0.6	asymmetric CH_3
	3074.7	12.9	asymmetric CH_3
	3053.1	725.0	bonded-NH(1)
	2989.0	18.1	symmetric CH_3
	2852.6	1246.8	bonded-NH(2)
	VII	3715.9	120.6
3712.0		111.0	free-OH(2) [Ad]
3706.4		131.6	antisymmetric free-OH(4) [aa]
3705.6		167.5	two-coordinated free-OH(1) [Ad]
3621.4		17.5	symmetric free-OH(4) [aa]
3526.4		373.5	bonded-OH(3) [ad]
3466.5		558.5	bonded-OH(1) [Ad]
3389.0		62.0	free-NH
3336.7		831.4	bonded-OH(2) [Ad]
3080.8		0.7	asymmetric CH_3
3077.0		2.6	asymmetric CH_3
3035.0		785.8	bonded-NH(1)
2990.0		29.3	symmetric CH_3
2867.5		1163.7	bonded-NH(2)
VIII		3741.9	118.1
	3728.9	131.3	antisymmetric free-OH(2) [A]
	3712.1	95.6	free-OH(1) [Ad]
	3704.7	101.0	free-OH(3) [ad]
	3647.5	26.9	symmetric free-OH(4) [a]
	3640.3	44.0	symmetric free-OH(2) [A]
	3401.8	622.8	bonded-OH(3) [ad]
	3388.4	56.2	free-NH
	3186.4	1124.6	bonded-OH(1) [Ad]
	3109.0	822.1	bonded-NH(2)
	3080.1	4.9	asymmetric CH_3
	3077.1	13.7	asymmetric CH_3
	2990.1	9.2	symmetric CH_3
	2803.6	1517.4	bonded-NH(1)
	IX	3738.0	121.5
3732.0		129.1	free-OH(2) [Ad]
3731.6		114.2	free-OH(4) [ad]
3709.8		103.7	antisymmetric free-OH(1) [Aa]

Table 4. Continued

	Frequency	Intensity	Assignments
	3644.9	28.1	symmetric free-OH(3) [A]
	3642.1	27.5	symmetric free-OH(1) [Aa]
	3641.7	52.0	bonded-OH(4) [ad]
	3376.6	723.7	bonded-OH(2) [Ad]
	3173.1	783.7	bonded-NH(1)
	3152.8	517.9	bonded-NH(3)
	3074.3	8.4	asymmetric CH ₃
	3073.3	4.1	asymmetric CH ₃
	3007.7	902.2	bonded-NH(2)
	2984.8	140.4	symmetric CH ₃
X	3713.3	145.0	free-OH(3) [Ad]
	3696.0	68.0	symmetric free-OH(1,2) [Aad,Aad]
	3692.8	220.3	antisymmetric free-OH(1,2) [Aad,Aad]
	3690.4	158.8	free-OH(4) [aad]
	3549.7	158.4	bonded-OH(2) [Aad]
	3507.0	387.8	asymmetric bonded-OH(1,3,4) [Aad,Ad,aad]
	3466.2	405.5	asymmetric bonded-OH(1,3,4) [Aad,Ad,aad]
	3448.1	143.0	symmetric bonded-OH(1,4) [Aad,aad]
	3279.0	167.6	bonded-NH(2)
	3191.4	346.6	bonded-NH(1)
	3076.2	1.9	asymmetric CH ₃
	3075.4	2.1	asymmetric CH ₃
	3016.9	720.5	bonded-NH(3)
	2987.5	54.9	symmetric CH ₃
XI	3730.4	131.1	antisymmetric free-OH(4) [a]
	3709.8	151.4	free-OH(3) [ad]
	3706.6	116.4	free-OH(2) [Ad]
	3681.2	96.4	free-OH(1) [Aad]
	3639.9	39.0	symmetric free-OH(4) [a]
	3508.6	329.3	bonded-OH(3) [ad]
	3388.0	72.9	free-NH
	3302.3	693.5	bonded-OH(2) [Ad]
	3273.2	1017.2	bonded-OH(1) [Aad]
	3079.7	11.5	antisymmetric CH ₃
	3077.0	55.6	antisymmetric CH ₃
	3065.5	644.8	bonded-NH(1)
	2989.3	9.2	symmetric CH ₃
	2794.0	1200.7	bonded-NH(2)

were determined at the centers of features, and those for shoulder (sh) features were determined by nonlinear least squares fits with multiple gaussian functions. Considering that each isomer possesses two or three b-NH stretches, the observation of nine b-NH stretch peaks suggests that multiple structural isomers are populated in our ion beam at 150 K. This result is different from the case of NH₄⁺(H₂O)₄ where only four b-NH stretch peaks were found.¹¹

The contributions from each structural isomer to the measured VP spectrum were determined by correlating the observed features with the *ab initio* predicted b-NH peaks of each isomer as shown in Figure 2. It was found that the observed vibrational features correlate excellently with the

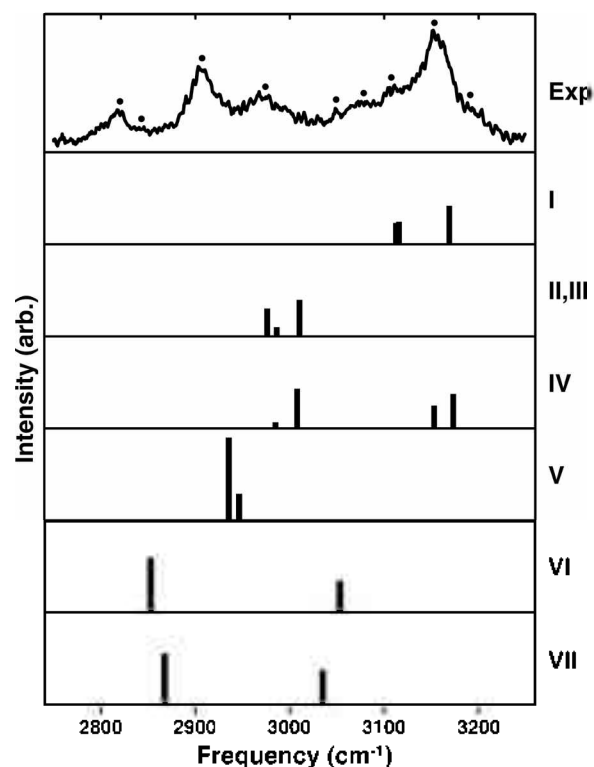


Figure 2. Vibrational predissociation spectrum and calculated stick spectra for b-NH stretches of structural isomers I-VII at B3LYP/6-311++G(d,p). The identified VP peaks are labeled by dots (•).

calculated b-NH stretches of seven isomers (I-VII) consistent with the trends of calculated Gibbs free energies at 150 K. The 2818 cm⁻¹ peak can be correlated with the b-NH(2) stretch of isomer VI (2853 cm⁻¹) and the broad peak at ~2840 cm⁻¹ correlates with the b-NH(2) stretch of isomer VII (2868 cm⁻¹). The intense feature at 2906 cm⁻¹ can be assigned to the combined symmetric and antisymmetric b-NH(1,2) stretches of isomer V (2935, 2946 cm⁻¹).

The broad feature at ~2972 cm⁻¹ and its shoulder in the high frequency side can be assigned to the mixed b-NH(1,2) stretches of isomer II, III (2976, 2986, 3010 cm⁻¹) and b-NH(1) stretches of isomer IV (2985, 3008 cm⁻¹). The 3049 cm⁻¹ peak correlates with the b-NH(1) of isomer VII (3035 cm⁻¹), and the shoulder feature at 3075 cm⁻¹ correlates with the b-NH(1) stretch of isomer VI (3053 cm⁻¹). The 3110 cm⁻¹ shoulder feature is assigned to the combined symmetric and antisymmetric b-NH(1,2) stretches of isomer I (3112, 3116 cm⁻¹). Finally, the 3154, 3196(sh) cm⁻¹ features are attributed to the mixed b-NH(3) stretch of isomer I (3169 cm⁻¹) and symmetric and antisymmetric b-NH(2,3) stretches of isomer IV (3153, 3173 cm⁻¹).

The excellent correlation between the observed and calculated spectra confirms the co-existence of seven isomers (I-VII) in our ion beam at 150 K consistent with the *ab initio* predictions, although minor contributions from other high energy isomers (VIII-XI) cannot be excluded due to the broadened vibrational features. The experimental identification of five cyclic isomers (I, II, III, VI, VII) besides two non-cyclic isomers (IV, V) for Ma(H₂O)₄ at 150 K is

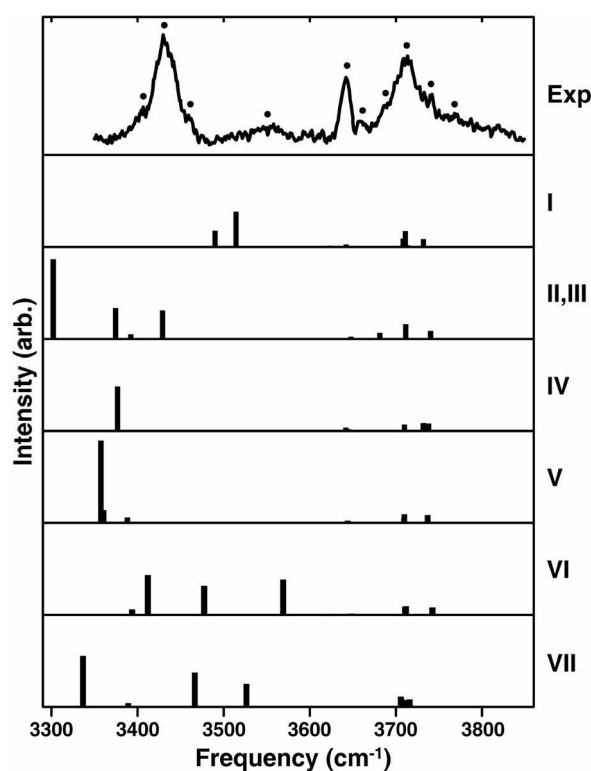


Figure 3. Vibrational predissociation spectrum and calculated stick spectra for b-OH, f-NH and f-OH stretches of structural isomers I-VII at B3LYP/6-311++G(d,p). The identified VP peaks are labeled by dots (•).

remarkable considering the fact that for $\text{NH}_4^+(\text{H}_2\text{O})_4$ at similar ion temperatures, only one cyclic and two non-cyclic isomers were identified.¹¹ The observed structural diversity for $\text{Ma}(\text{H}_2\text{O})_4$ at 150 K may originate from the decreased charge densities of protons by methyl substitution resulting in less energy discrepancies between charge-dipole and water-water HB interactions. The asymmetric hydration around $-\text{NH}_3$ moiety in Ma core by the presence of hydrophobic $-\text{CH}_3$ group permitting closer water-water interactions may also contribute to the structural diversity.

Bonded O-H and free O-H stretches: Figure 3 depicts the observed and calculated spectra for b-OH and f-OH stretches in the frequency range of 3300–3850 cm^{-1} . Note that the spectral features in the 3250–3350 cm^{-1} region are omitted due to strong background absorption by crystal surfaces. Different from the cases of b-NH stretches, only four vibrational features for b-OH stretches in the 3300–3600 cm^{-1} region were identified in the VP spectrum: 3406(sh), 3430, 3460(sh), ~3550(br). As illustrated in Figure 3 and Table 4, the f-NH stretches for isomers with two ion-water HB's (II, III, V, VI, VII) are predicted to have much lower IR intensities than b-OH stretches, so their contributions to the observed spectrum were ignored in this work. The correlation between the observed and calculated stick spectra (Figure 3) suggests that several b-OH stretches of isomers I-VII are highly mixed.

The 3406(sh), 3430 cm^{-1} features may be assigned to the mixed b-OH stretches of isomers II-VI: symmetric and

antisymmetric b-OH(1,2) of II, III (3374, 3428 cm^{-1}), b-OH(1) of IV (3377 cm^{-1}), symmetric and antisymmetric b-OH(1,2) of V (3357, 3361 cm^{-1}), and b-OH(2) of VI (3412 cm^{-1}). The shoulder feature at 3460 cm^{-1} correlates with the mixed b-OH(1) stretch of VI (3477 cm^{-1}) and b-OH(1) stretch of VII (3467 cm^{-1}). The ~3550 cm^{-1} feature is generally considered as signature for 4-HB cyclic isomer I,¹¹ thus assigned primarily to the mixed symmetric and antisymmetric b-OH(1,2) stretches of I (3490, 3514 cm^{-1}) with some contributions from b-OH(2) stretch of VI (3569 cm^{-1}) and b-OH(3) stretch of VII (3526 cm^{-1}). The observed spectral congestion for b-OH stretches, different from the cases of b-NH stretches, could be due to the facile rearrangements between structural isomers with the same number of ion-water HB's (*i.e.* I, IV and II, III, V, VI, VII) involving water-water HB breaking and formation, migrations of water molecules as mentioned previously.

On the other hand, the f-OH stretch frequencies are predicted to be insensitive to the types of structural isomers but rather sensitive to the HB roles of water molecules within each isomer as illustrated in Figure 3 and Table 4. The predicted f-OH stretch frequency of three-coordinated aad-2° $\text{H}_2\text{O}(3)$ in II, III is 3681 cm^{-1} while those for two-coordinated Ad-1° H_2O in isomers I-VII appear in 3706–3713 cm^{-1} range. Moreover, the symmetric and antisymmetric f-OH stretches for two-coordinated aa-2° H_2O (I, VI, VII) appear in 3621–3627 cm^{-1} and 3706–3711 cm^{-1} ranges, respectively. The symmetric and antisymmetric f-OH stretch frequencies for one-coordinated A-1° H_2O (*i.e.* N-H...OH₂) (I, IV) are ~3642 cm^{-1} and ~3732 cm^{-1} , and those for a-2°, 3° H_2O (*i.e.* O-H...OH₂) (II-VI) are 3644–3648 cm^{-1} and 3737–3742 cm^{-1} , close to those of isolated H_2O (3636, 3756 cm^{-1}). The similar trends for distinct f-OH stretch frequencies depending on the HB roles of water molecules but not much on the hydration shells and the types of isomers, have been reported previously.¹⁸ This suggests that the f-OH stretch peaks can be also used as fingerprints for identifying the structural isomers and in particular, the HB roles of water molecules in diverse hydration environments.

Six f-OH stretch peaks were identified in the VP spectrum: 3642, 3658, 3688(sh), 3710, 3736(sh), ~3760(br) cm^{-1} . According to the predicted trends for f-OH stretches, the 3642 cm^{-1} peak is correlated with mixed symmetric f-OH stretches for A-1° H_2O of isomers I, IV, and a-2°, 3° H_2O of isomers II-VI. The 3710 cm^{-1} peak correlates with the mixed f-OH stretches for Ad-1° H_2O in isomers I-VII, and antisymmetric f-OH stretches for aa-2° H_2O of isomers I, VI, VII. The 3688(sh) cm^{-1} feature can be assigned exclusively to the three-coordinated f-OH stretches for aad-2° $\text{H}_2\text{O}(3)$ in isomers II, III. The 3736(sh), ~3760(br) cm^{-1} features are assigned to the mixed antisymmetric f-OH stretches for A-1° H_2O (I, IV) and a-2°, 3° H_2O (II-VI) containing some internal rotation progressions as reported previously.¹¹ Finally, the 3658 cm^{-1} feature, not seen in the cases of $\text{NH}_4^+(\text{H}_2\text{O})_n$, may be due to the internal rotation progressions for A-1° H_2O molecules or overtones, combination bands involving low frequency modes.

Conclusions

In this paper we described the combined *ab initio* and vibrational predissociation spectroscopic studies on methylammonium-(water)₄ complex aimed at understanding the hydration behavior of an amphiphilic ion core. *Ab initio* calculations predicted eleven low energy isomers forming cyclic, tripod, chain, and caged structures, and also their relative stabilities, hydration energies, and thermodynamic functions. The trends for the calculated Gibbs free energies at 150 K suggested significant populations of multiple cyclic and non-cyclic isomers in our ion beam, different from the case of ammonium-(water)₄ complex. The excellent correlation between the observed vibrational predissociation spectra and calculated spectra for bonded N-H, bonded O-H and free O-H stretches of seven structural isomers (I-VII) corroborated the theoretical predictions.

Acknowledgements. This work was supported by Korea Research Foundation Grant (KRF-2003-015-C00281), Korea.

References

- Orozco, M.; Luque, F. J. *Chem. Rev.* **2000**, *100*, 4187.
- Desfrancois, C.; Carles, S.; Schermann, J. P. *Chem. Rev.* **2000**, *100*, 3943.
- Cheng, Y. K.; Rossky, P. J. *Nature* **1998**, *392*, 696.
- Mao, Y.; Ratner, M. A.; Jarrold, M. F. *J. Am. Chem. Soc.* **2000**, *122*, 2950.
- Christie, R. A.; Jordan, K. D. *J. Phys. Chem. A* **2001**, *105*, 7551.
- Kim, K. Y.; Cho, U. I.; Boo, D. W. *Bull. Kor. Chem. Soc.* **2001**, *22*, 597.
- Meot-Ner, M.; Scheiner, S.; Yu, W. O. *J. Am. Chem. Soc.* **1998**, *120*, 6980.
- Klassen, J. S.; Blades, A. T.; Kebarle, P. J. *J. Phys. Chem.* **1995**, *99*, 15509.
- Wu, C. C.; Jiang, J. C.; Boo, D. W.; Lin, S. H.; Lee, Y. T.; Chang, H. C. *J. Chem. Phys.* **2000**, *112*, 176.
- Jiang, J. C.; Chang, H. C.; Lee, Y. T.; Lin, S. H. *J. Phys. Chem. A* **1999**, *103*, 3123.
- Wang, Y. S.; Chang, H. C.; Jiang, J. C.; Lin, S. H.; Lee, Y. T.; Chang, H. C. *J. Am. Chem. Soc.* **1998**, *120*, 8777.
- Frisch, M. J. *et al.*, GAUSSIAN 98 (Revision A.7); Gaussian, Inc.: Pittsburgh, PA, 2001.
- Boys, S. F.; Bernardi, F. *Mol. Phys.* **1970**, *19*, 553.
- Boo, D. W.; Lee, Y. T. *J. Chem. Phys.* **1995**, *103*, 520.
- Meot-Ner, M. *J. Am. Chem. Soc.* **1984**, *106*, 1265.
- Lee, S.-W.; Cox, H.; Goddard, W. A., III; Beauchamp, J. L. *J. Am. Chem. Soc.* **2000**, *122*, 9201.
- Kim, K. Y.; Cho, U. I.; Boo, D. W., submitted for publication in *Chem. Phys. Lett.* **2006**.
- The proton acceptor roles for protons of Ma core and another water molecules are distinguished by the letters A and a, respectively.
- Wang, Y. S.; Jiang, J. C.; Cheng, C. L.; Lin, S. H.; Lee, Y. T.; Chang, H. C. *J. Chem. Phys.* **1997**, *107*, 9695.